Supplement to: Upscaling Northern Peatland CO₂ Fluxes Using Satellite Remote Sensing Data

Sofia Junttila[1], Julia Kelly[2], Natascha Kljun[2], Mika Aurela[3], Leif Klemedtsson[4], Annalea Lohila[3, 5], Mats B. Nilsson[6], Janne Rinne[1], Eeva-Stiina Tuittila[7], Patrik Vestin[1], Per Weslien[4] and Lars Eklundh[1]

[1] Department of Physical Geography and Ecosystem Science, Lund University, 223 62 Lund, Sweden
[2] Centre for Environmental and Climate Science, Lund University, 223 62 Lund, Sweden
[3] Finnish Meteorological Institute, Erik Palménin aukio 1, 00560, Helsinki, Finland
[4] Department of Earth Sciences, University of Gothenburg, 405 30 Gothenburg, Sweden
[5] Institute for Atmospheric and Earth System Research (INAR) / Physics, P.O. Box 64, 00014 University of Helsinki, Finland
[6] Department of Forest Ecology and Management, Swedish University of Agricultural Sciences, 901 83 Umeå, Sweden
[7] School of Forest Sciences, University of Eastern Finland, 80101 Joensuu, Finland

1. *Eddy covariance flux data processing*

At Abisko-Stordalen, Lompolojänkkä, Degerö and Siikaneva, site instrumentation and flux data processing followed the ICOS recommendations [1, 2].

At Mycklemossen, the CO₂ flux measurements were performed using an EC system consisting of a LI-7200 closed path gas analyzer (Li-COR Inc., Lincoln, NE, USA) and a USA-1 sonic anemometer (METEK Gmbh, Elmshorn, Germany). The EC system was mounted at 2.4 m height on a mast located centrally at within the peatland. The intake tube for the gas analyzer was heated, insolated and protected by a filter close to the air intake. Measurements were performed at 10 Hz. EC fluxes were calculated using the EddyPro software (version 6.2.1, LI-COR, Lincoln, NE, USA) for half-hourly intervals. Turbulent fluctuations from the mean were extracted using block averaging. Anemometer data was corrected for tilt by double rotation and for cross-wind. Raw data screening according to Vickers and Mahrt [3] was performed. Spectral corrections were applied according to Moncrieff, et al. [4] and Horst [5]. The Mauder and Foken [6] quality test on developed turbulent conditions and steady-state conditions were applied to the half-hourly flux data.

2. The multivariate linear regression model for NEE

To improve the modelling results of NEE, we tested a purely empirical NEE model. A multiple linear regression model with EVI2, NDWI, LST, PPFD, WTD and W_s as predictor variables was fitted against EC NEE measurements.

$$NEE = b_1 + b_2 \times EVI2 + b_3 \times NDWI + b_4 \times LST + b_5 \times PPFD + b_6 \times WTD + b_7 \times W_s. \quad (1)$$

Following the main analysis, the free parameters were derived 1) for each site separately, and 2) jointly for all the sites with the LOOCV method. The linear NEE model with the average (LOOCV) parameters performed similar or even poorer than the mechanistic NEE model (Eq. 9) at Abisko-Stordalen, Lompolojänkkä and Degerö but slightly better at Siikaneva (R^2 = 0.51, RMSE = 0.36 μmol m⁻² s⁻¹, NRMSE = 13%) and Mycklemossen (R^2 = 0.15, RMSE = 0.37 μmol m⁻² s⁻¹, NRMSE = 14%).

Table S1. TIMESAT spline parameters

Data	Spline smoothing factor	Spline adaptation factor	No. of envelope interations
Sentinel-2 EVI2	1000	0.5	2
Sentinel-2 NDWI	1000	0.5	2
MODIS LST	1	1	1
EC flux data	1	1	1

Table S2. Coefficient of determination (R^2) between the EC-derived GPP and ER, environmental data, and remote sensing-derived indices using all sites and available years. Sum denotes the annual cumulative sum of the variable; peak denotes the annual 99-percentile of the variable. Min and mean denotes the annual minimum and average of the variable, respectively. Precip sum is the annual precipitation measured at the site; precip spring denotes the precipitation measured from January to June at the site.

	GPP sum	GPP peak	ER sum	ER peak	EVI2 peak	NDWI peak	Ws	Precip sum	Precip spring sum	WTD min	WTD mean	Tair sum	Tair mean	PPFD mean
GPP sum	1.00	0.59	0.85	0.73	0.02	0.00	0.00	0.19	0.15	0.29	0.29	0.25	0.25	0.23
GPP peak		1.00	0.32	0.40	0.21	0.10	0.10	0.15	0.00	0.09	0.09	0.02	0.02	0.02
ER sum			1.00	0.87	0.02	0.06	0.06	0.26	0.28	0.33	0.33	0.51	0.51	0.45
ER peak				1.00	0.05	0.06	0.06	0.25	0.18	0.25	0.25	0.36	0.36	0.31
EVI2 peak					1.00	0.04	0.04	0.00	0.01	0.12	0.11	0.19	0.19	0.03
NDWI peak						1.00	1.00	0.06	0.14	0.18	0.18	0.31	0.31	0.20
Ws							1.00	0.06	0.14	0.18	0.18	0.31	0.31	0.20
Rain sum								1.00	0.75	0.00	0.00	0.02	0.02	0.28
Rain spring sum									1.00	0.00	0.00	0.29	0.29	0.40
WTD min										1.00	1.00	0.21	0.21	0.01
WTD mean											1.00	0.21	0.21	0.01
Tair sum												1.00	1.00	0.32
Tair mean													1.00	0.31
PPFD mean														1.00

Table S3. R^2 and NRMSE (in brackets, normalized using the range of the EC-derived ER) of the ER models at each site. The models were fitted to all available years. W_s = NDWI scalar, E_s = EVI2 scalar, formulated in the same way as W_s. Models with W_s or E_s are the original model equation multiplied by the respective scalar. The Gao et al. (2015) model was also fit separately for the dormant and growing season ('2 seasons').

Site	Lloyd and Taylor (1994)			Heskel et al. (2016)			Gao et al. (2015)			
	Original	Ws	Es	Original	Ws	Es	Original	Ws	Es	2 seasons
SE-Sto	0.71 (11.5)	0.72 (11.2)	0.78 (10.1)	0.78 (9.3)	0.78 (9.3)	0.78 (9.2)	0.86 (8.0)	0.86 (7.9)	0.86 (8.0)	0.86 (7.8)
FI-Lom	0.82 (10.7)	0.84 (10.1)	0.90 (8.1)	0.74 (11.3)	0.74 (11.4)	0.74 (11.3)	0.91 (7.4)	0.92 (7.2)	0.92 (7.1)	0.93 (6.6)
SE-Deg	0.77 (11.6)	0.76 (11.9)	0.79 (11.1)	0.84 (9.8)	0.84 (9.8)	0.85 (9.8)	0.79 (11.2)	0.77 (11.7)	0.80 (11.1)	0.80 (11.0)
FI-Sii	0.86 (9.4)	0.86 (9.3)	0.90 (8.0)	0.85 (9.9)	0.85 (9.9)	0.85 (9.8)	0.91 (7.4)	0.90 (7.8)	0.92 (7.2)	0.92 (7.1)
SE-Myc	0.77 (12.4)	0.77 (12.2)	0.77 (12.3)	0.69 (11.8)	0.69 (11.7)	0.69 (11.7)	0.81 (11.1)	0.81 (11.2)	0.80 (11.3)	0.83 (10.5)

Table S4. Site-specific model parameters

Site	GPP	ER			NEE				
	a	Ref	E0	a	Rref	E0	b1	b2	
SE-Sto	0.55	0.25	180	4.86	0.0003	2162	5.27	0.46	
FI-Lom	1.00	1.04	184	6.91	0.0225	1130	25.71	1.47	
SE-Deg	0.65	0.32	350	4.02	0.0005	1668	4.78	0.37	
FI-Sii	0.53	0.54	248	4.30	0.0001	1812	7.35	0.40	
SE-Myc	1.19	0.48	451	10.80	0.0079	1073	10.69	0.58	

Table S5. The prediction performance of the GPP model during the leave-one-out-cross-validation runs. The model parameter a was estimated excluding one site-year and validated against data from the excluded site-year.

Site excluded	Year excluded	a	R²	RMSE (μmol m⁻² s⁻¹)	NRMSE (%)
SE-Sto	2017	0.70	0.90	0.31	7
SE-Sto	2018	0.72	0.47	0.53	21
SE-Sto	2019	0.71	0.71	0.44	14
FI-Lom	2017	0.67	0.78	0.87	12
FI-Lom	2018	0.66	0.71	1.22	14
SE-Deg	2017	0.69	0.76	0.53	14
SE-Deg	2018	0.70	0.83	0.32	14
SE-Deg	2019	0.72	-0.17	0.59	28
FI-Sii	2017	0.73	0.65	0.67	18
FI-Sii	2018	0.71	0.85	0.41	12
FI-Sii	2019	0.74	0.53	0.85	21
SE-Myc	2017	0.68	0.54	0.96	22
SE-Myc	2018	0.68	0.47	0.95	21
	Mean	**0.70**	**0.62**	**0.67**	**17**
	std	**0.02**	**0.27**	**0.27**	**5**

Table S6. The prediction performance of the ER model during the leave-one-out-cross-validation runs. The model parameters (Rref, E0, and a) were estimated excluding one site-year and validated against data from the excluded site-year.

Site excluded	Year excluded	Rref	E0	a	R²	RMSE (μmol m⁻² s⁻¹)	NRMSE (%)
SE-Sto	2017	0.58	294	4.5	0.57	0.36	16
SE-Sto	2018	0.57	292	4.9	-0.47	0.51	31
SE-Sto	2019	0.58	288	4.7	-0.14	0.44	23
FI-Lom	2017	0.54	324	3.6	0.66	0.58	17
FI-Lom	2018	0.53	320	3.7	0.57	0.77	18
SE-Deg	2017	0.58	296	4.2	0.87	0.24	10
SE-Deg	2018	0.6	298	4.0	0.79	0.33	13
SE-Deg	2019	0.61	299	4.1	-2.16	0.65	42
FI-Sii	2017	0.56	305	4.6	0.74	0.35	16
FI-Sii	2018	0.52	334	4.4	0.8	0.38	12
FI-Sii	2019	0.54	315	4.7	0.87	0.3	11
SE-Myc	2017	0.45	350	4.4	0.36	0.92	24
SE-Myc	2018	0.53	232	5.7	0.36	1.27	23
	Mean	**0.55**	**304**	**4.4**	**0.29**	**0.55**	**20**
	std	**0.04**	**27**	**0.5**	**0.81**	**0.28**	**9**

Table S7. The prediction performance of the NEE model during the leave-one-out-cross-validation runs. The model parameters (Rref, E0, b1, b2) were estimated excluding one site-year and validated against data from the excluded site-year.

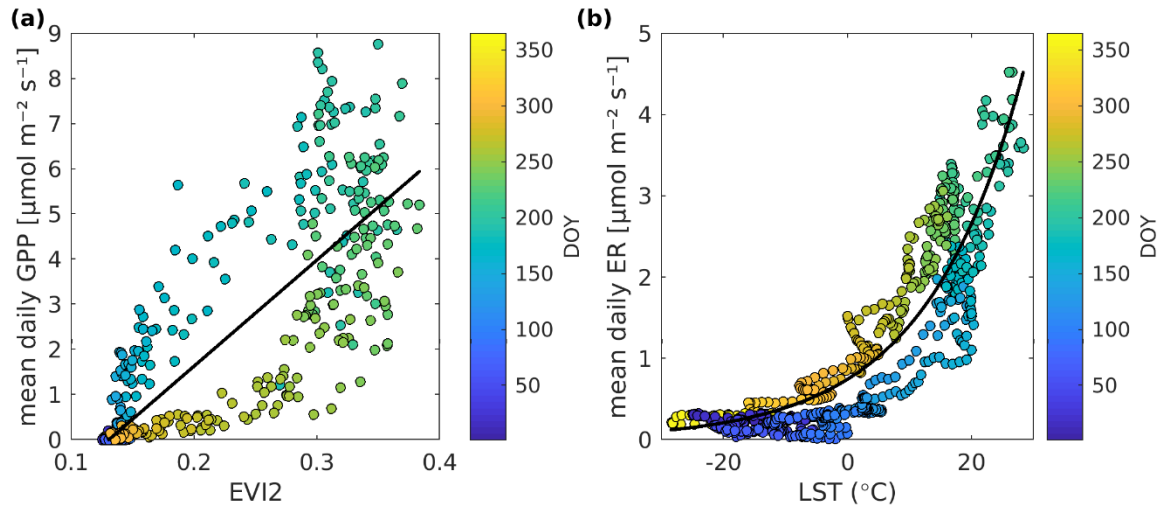| Site excluded	Year excluded	Rref	E0	b1	b2	R^2	RMSE (μmol m^{-2} s^{-1})	NRMSE (%)
SE-Sto	2017	0.011	1049	10.0	0.64	0.51	0.35	14
SE-Sto	2018	0.013	1018	9.4	0.63	0.64	0.19	14
SE-Sto	2019	0.017	970	9.4	0.63	0.56	0.25	12
FI-Lom	2017	0.005	1174	8.1	0.54	0.52	0.72	12
FI-Lom	2018	0.009	1079	6.6	0.48	0.49	0.97	15
SE-Deg	2017	0.025	884	8.8	0.62	0.42	0.40	16
SE-Deg	2018	0.014	1007	9.2	0.62	0.21	0.24	15
SE-Deg	2019	0.011	1065	10.0	0.66	-0.61	0.31	26
FI-Sii	2017	0.018	962	9.3	0.65	0.58	0.32	15
FI-Sii	2018	0.013	1026	9.0	0.61	0.15	0.39	19
FI-Sii	2019	0.020	956	10.7	0.72	-0.31	0.57	26
SE-Myc	2017	0.012	1034	8.8	0.61	-0.10	0.46	17
SE-Myc	2018	0.010	1087	9.0	0.61	-0.01	0.35	15
	Mean	**0.014**	**1024**	**9.1**	**0.62**	**0.23**	**0.43**	**17**
	std	**0.005**	**70**	**1.0**	**0.05**	**0.38**	**0.21**	**4**

Figure S1. Example of the relationship between (a) EVI2 and EC-derived GPP and (b) LST and EC-derived ER, from Lompolojänkkä (2017-2018) that shows differences between the first and second half the year. Black lines are (a) linear and (b) exponential regression fits

Table S8. Annual cumulative NEE (g C m^{-2}) for the TIMESAT smoothed NEE (EC), the non-linear regression model of NEE with joint parameters (RS joint) and the non-linear regression model of NEE with site-specific parameters (RS site).

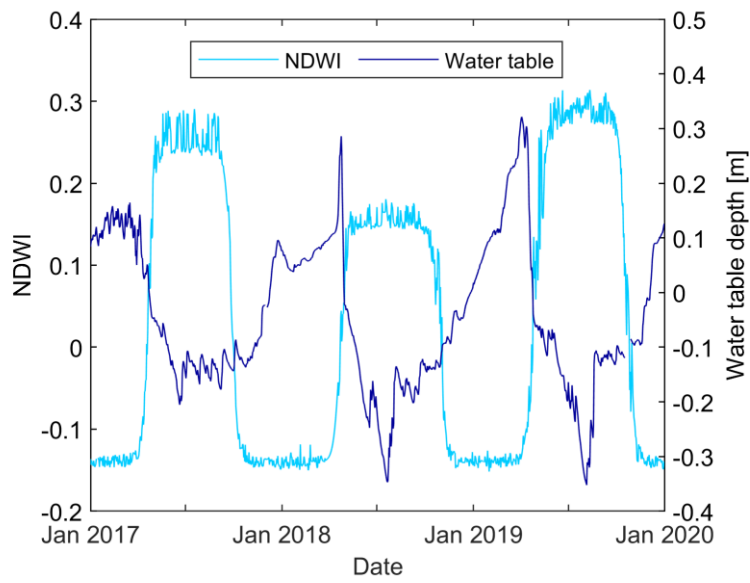| Site	Year	NEE-EC	NEE-RS (joint)	NEE-RS (site)
		g C m^{-2}	g C m^{-2}	g C m^{-2}
SE-Sto	2017	-35	2	-36
SE-Sto	2018	-26	-26	-52
SE-Sto	2019	-31	-16	-43
FI-Lom	2017	-29	-49	-46
FI-Lom	2018	-56	-80	-120
SE-Deg	2017	-75	-38	-42
SE-Deg	2018	15	21	-7
SE-Deg	2019	-11	-30	-42
FI-Sii	2017	-54	-105	-53
FI-Sii	2018	21	-15	-18
FI-Sii	2019	-24	-100	-54
SE-Myc	2017	41	-37	-5
SE-Myc	2018	55	15	23

Figure S2. Example of NDWI (Normalized Difference Water Index) and water table depth time series at Degerö.
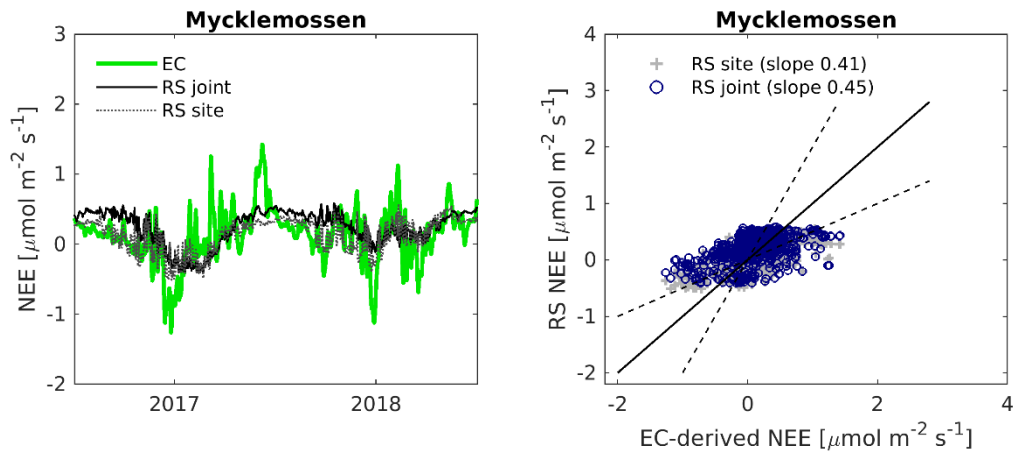

Figure S3. Example of the multivariate linear regression model for NEE (Eq. S1) at Mycklemossen.

References

1. Rebmann, C.; M. Aubinet; H. Schmid; N. Arriga; M. Aurela; G. Burba; R. Clement; A. De Ligne; G. Fratini; B. Gielen; J. Grace; A. Graf; P. Gross; S. Haapanala; M. Herbst; L. Hörtnagl; A. Ibrom; L. Joly; N. Kljun; O. Kolle; A. Kowalski; A. Lindroth; D. Loustau; I. Mammarella; M. Mauder; L. Merbold; S. Metzger; M. Mölder; L. Montagnani; D. Papale; M. Pavelka; M. Peichl; M. Roland; P. Serrano-Ortiz; L. Siebicke; R. Steinbrecher; J.-P. Tuovinen; T. Vesala; G. Wohlfahrt; D. Franz. Icos Eddy Covariance Flux-Station Site Setup: A Review. *International Agrophysics* **2018**, *32*, no. 4: 471-494.
2. Sabbatini, S.; I. Mammarella; N. Arriga; G. Fratini; A. Graf; L. Hörtnagl; A. Ibrom; B. Longdoz; M. Mauder; L. Merbold; S. Metzger; L. Montagnani; A. Pitacco; C. Rebmann; P. Sedlák; L. Šigut; D. Vitale; D. Papale. Eddy Covariance Raw Data Processing for Co2 and Energy Fluxes Calculation at Icos Ecosystem Stations. *International Agrophysics* **2018**, *32*, no. 4: 495-515.
3. Vickers, D.; L. Mahrt. Quality Control and Flux Sampling Problems for Tower and Aircraft Data. *Journal of atmospheric and oceanic technology* **1997**, *14*, no. 3: 512-526.
4. Moncrieff, J.; R. Clement; J. Finnigan; T. Meyers. Averaging, Detrending, and Filtering of Eddy Covariance Time Series. In *Handbook of Micrometeorology*, 7-31: Springer, 2004.
5. Horst, T. A Simple Formula for Attenuation of Eddy Fluxes Measured with First-Order-Response Scalar Sensors. *Boundary-Layer Meteorology* **1997**, *82*, no. 2: 219-233.
6. Mauder, M.; T. Foken. Documentation and Instruction Manual of the Eddy-Covariance Software Package Tk3. **2011**.